

Atomic Structure of Cu Adlayers on Au(100) and Au(111) Electrodes Observed by *In Situ* Scanning Tunneling Microscopy

O. M. Magnussen, J. Hotlos,^(a) R. J. Nichols,^(b) D. M. Kolb,^(b) and R. J. Behm

*Institut für Kristallographie und Mineralogie, Universität München,
Theresienstrasse 41, D-8000 München 2, Federal Republic of Germany*

(Received 6 February 1990)

The atomic structure of ordered Cu adsorbate layers on Au(111) and Au(100) electrode surfaces and of the clean substrates was resolved in scanning tunneling microscopy images taken *in situ*. For sub-monolayer coverages deposited from sulfuric acid solutions under potential control, various ordered structures were observed. The quasihexagonal arrangement of Cu atoms in these structures reflects increasingly repulsive interactions between closely spaced Cu adatoms. These structures differ from the pseudomorphic Cu adlayer formed under vacuum conditions, which demonstrates the structure-determining role of the coadsorbed anions.

PACS numbers: 68.55.-a, 61.16.Di

Structure and growth of metal adlayers, which constitute the first step for deposition and growth of thin metal films, have been investigated thoroughly for gas-phase-deposited adlayers. The situation is quite different for the technically important and widely used case of electrochemical deposition from an aqueous solution. Classical electrochemical methods inherently are not very structure sensitive, and the exact atomic arrangement of adlayers on electrodes could only be derived from *ex situ* measurements, e.g., by LEED or reflection high-energy electron diffraction (RHEED), after the sample had been removed from the electrolyte.^{1,2} Only very recently has structural information become accessible from *in situ* extended x-ray-absorption fine-structure experiments,³ and *in situ* scanning tunneling microscopy (STM) measurements.⁴⁻⁶ We here present results from an STM study on the deposition under potential of sub-monolayer amounts of Cu on Au(111) and Au(100) electrodes, for which images with atomic resolution from the clean and Cu-covered substrate were obtained *in situ*. These images allow direct access to the atomic structure of the surface. Our data reveal a general tendency of these adlayers to arrange in well-ordered, quasihexagonal structures, which are most likely caused by repulsive interactions within the adlayer due to the presence of coadsorbed anions.

The experiments were performed in a pocket-size STM which was modified for *in situ* electrochemical studies, as described in detail by Wiechers *et al.*⁷ The potential of the Au single-crystal electrode was measured against a saturated calomel electrode (SCE). Because the tip acts as a fourth electrode, its potential U_t was held constant with respect to the reference electrode, at a level which minimizes faradic currents and chemical processes on the tip. Consequently different sample potentials, as applied during the deposition process, resulted in different tunnel voltages which, however, had little influence on the STM images. To further reduce faradic processes at the tungsten tip, it was covered by a thin

layer of a thermoplast (Apiezon wax) except for the foremost $\sim 10 \mu\text{m}$. Before each electrochemical experiment, the Au electrodes were prepared by the so-called flame annealing method⁸ which led to a well-ordered surface with atomically flat terraces.⁷ The electrolyte was 0.05 M H_2SO_4 + 5 mM CuSO_4 made of H_2SO_4 (suprapure, Merck), CuSO_4 (p.a., Merck), and triply distilled water.

Preliminary STM measurements revealed that Cu adsorption-desorption cycles left the surface topography unchanged. Prior to Cu deposition, images of the clean gold surfaces were recorded at potentials positive relative to the onset of any Cu deposition. For Au(100) atomic resolution was reproducibly obtained for low gap resistances. These images showed the square lattice of the unreconstructed surface, with neighboring Au atoms 2.9 Å apart (Fig. 1). For Au(111), however, atomic resolution was not achieved and a relatively high level of back-

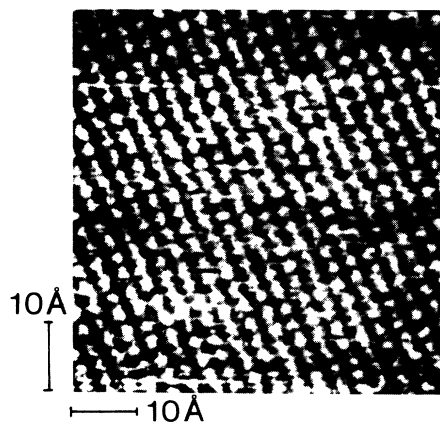


FIG. 1. Atomic-resolution STM image of the clean, unreconstructed Au(100) surface in 0.05 M H_2SO_4 + 5 mM CuSO_4 (atomic corrugation 0.5 Å, $U_t = -60$ mV, $I_t = 250$ nA, $U_{\text{SCE}} = 0.3$ V).

ground noise was always observed under these conditions. The failure to detect atomic structures on the bare Au(111) surface is attributed to the presence of adsorbed, mobile sulfate ions which are known to interact much stronger with Au(111) than with Au(100).⁹

Cu deposition was studied in sequences of STM measurements at stepwise more cathodic potentials. For Au(111) no new features were detected at potentials down to +0.22 V, i.e., the onset of the first pronounced deposition peak in the current-potential curves [see Fig. 2(a) in Ref. 10]. At this point a strongly corrugated, hexagonal superstructure covering most of the surface became visible (phase I). Simultaneously small areas of the surface appeared where this structure was absent but which exhibited significantly less noise than the clean Au(111) surface. Closer inspection revealed the presence of a second ordered phase at these places with a likewise hexagonal structure but a much weaker corrugation (phase II). Keeping the potential at +0.22 V, subsequent STM images showed the area covered by the strongly corrugated phase I to slightly decrease with time, and a concomitant expansion of the weakly corrugated phase II, until after several minutes equilibrium was reached. Lowering the potential by only 15 mV—to 0.20 V—led to the conversion of large parts of phase I into the weakly corrugated phase II. At potentials below 0.20 V this conversion was completed and in the entire potential range between 0.20 and 0.10 V only the phase

II was observed. This structural behavior is illustrated in the images in Fig. 2, which were part of a series of nine subsequent STM images taken at the same surface area at various potentials. They exhibit a sequence of atomically flat terraces separated by monoatomic steps. Each terrace is colored in its own grey scale for better contrast. In the upper image [Fig. 2(a)], taken after several minutes at a potential of 0.215 V, most of the surface area is covered by the strongly corrugated phase I. The lower image [Fig. 2(b)] depicts the same area after the potential was changed to 0.20 V. Large fractions of the middle terraces are now covered by the weakly corrugated phase II which is identified by a one-dimensional corrugation, at an angle of 30° to the lattice directions of the strongly corrugated phase I.

For the strongly corrugated structure of phase I (corrugation amplitude typically 0.5 Å) the distance of 4.9 ± 0.2 Å between the hexagonally ordered maxima is in perfect agreement with a $(\sqrt{3} \times \sqrt{3})R30^\circ$ superstructure, as has been found in recent *ex situ* LEED investigations for a Cu-covered Au(111) surface.² Associating the maxima with adsorbed Cu atoms, this superstructure corresponds to a Cu coverage of 0.33 monolayer (ML).

The corrugation of the second structure, which was barely resolved in Fig. 2(b), is enhanced by using higher tunnel currents (~ 100 nA) and consequently closer tip-surface distances [Fig. 3(a)]. In this image individual adatoms are resolved, in contrast to Fig. 2(b) where only a one-dimensional corrugation is discernible. Again the maxima are arranged hexagonally, but the distance between neighboring maxima is reduced to 3.6 ± 0.2 Å and the lattice directions are rotated by 30° with respect to those of the $(\sqrt{3} \times \sqrt{3})R30^\circ$ structure (see Fig. 2). Even under these conditions the corrugation amplitude (~ 0.3 Å) is much weaker than that of phase I. In this image a second, more long-range modulation is also resolved, with maxima four lattice constants of the superstructure apart, along its lattice directions. From the known geometry and orientation of the Au(111) substrate, the latter being determined by the $(\sqrt{3} \times \sqrt{3})R30^\circ$ superstructure, the corrugation of phase II can be assigned to a densely packed hexagonal structure of Cu adatoms in a

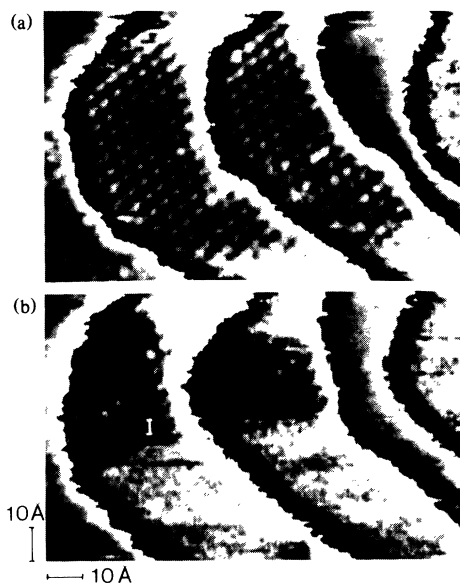


FIG. 2. STM images of a Cu-covered Au(111) surface in 0.05 M $\text{H}_2\text{SO}_4 + 5$ mM CuSO_4 , taken on the same area at slightly different potentials. (a) $U_{\text{SCE}} = 0.215$ V; (b) $U_{\text{SCE}} = 0.20$ V. Two Cu adlayer structures—a strongly corrugated $(\sqrt{3} \times \sqrt{3})R30^\circ$ and a weakly corrugated (5×5) —coexist on the surface ($U_t = -170$ mV, $I_t = 2.5$ nA, phases I and II as indicated).

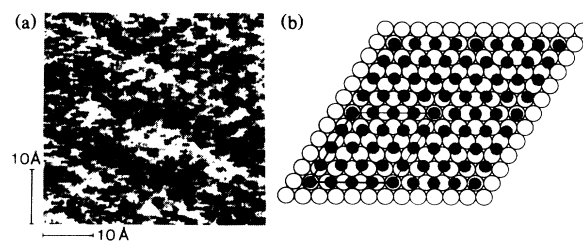


FIG. 3. (5×5) structure of a Cu adlayer on Au(111) in 0.05 M $\text{H}_2\text{SO}_4 + 5$ mM CuSO_4 at $U_{\text{SCE}} = 0.20$ V. (a) STM image ($U_t = -100$ mV, $I_t = 100$ nA); (b) model of the adlayer structure (○: Au atoms in the topmost layer; ●: Cu adatoms).

(5×5) unit cell, as is shown in Fig. 3(b). Here sixteen Cu atoms per unit cell result in an ideal coverage of 0.64 ML. Because of the mismatch between the hexagonal lattices of substrate and adsorbate only a part of the adsorbed Cu atoms are in registry with the substrate lattice, e.g., in threefold hollow sites. The other ones are forced onto more protruding bridge or top sites, which leads to the observed modulation along the lattice directions. Both the periodicity and the orientation of the long-range modulation as well as the atomic distance of 3.6 \AA agree completely with the (5×5) structural model proposed in Fig. 3(b).

For Cu deposition on Au(100) a sequence of ordered adlayers with similar structures was found at potentials between 0.25 and 0.15 V, and these are closely related to the structure shown in Fig. 3 for Au(111). The corrugation pattern in these STM images again reveals an almost hexagonal arrangement of Cu atoms. One of the lattice directions coincides with a substrate lattice direction. Along this $[1\bar{1}0]$ direction the maxima are well aligned. The distance between next-neighbor Cu atoms within the rows is $4.5 \pm 0.2 \text{ \AA}$, and adjacent rows are 2.9 \AA apart from each other, identical to the substrate lattice spacing in that direction. The two other lattice directions of the adlayer are often less well developed; they are oriented at angles of 50° and 70° , respectively, to the $[1\bar{1}0]$ direction. At 0.25 V, the Cu atoms are not exactly aligned along these directions, but exhibit a slight lateral modulation. Reducing the potential to 0.20 V causes a slight lateral reordering. The adlayer appears now well aligned in all three lattice directions, and the angles between lattice directions are changed to 45° and 75° , respectively [Fig. 4(a)]. Nevertheless, the angular distortions and differences in the distances between neighboring rows in different orientations make this structure different from a real hexagonal arrangement. Finally, around 0.18 V, concomitant with a sharp current peak in the cyclic voltammogram [see Fig. 2(c) in Ref. 10], this structure is abruptly destroyed and further uptake of

small amounts of Cu leads to a new structure. The characteristic arrangement of Cu atoms in well-aligned rows along the $[1\bar{1}0]$ lattice directions of the Au(100) substrate is maintained, but the Cu atoms are more compressed now within these rows.

The Cu adlayer structures on Au(100) are not as well-defined as those on Au(111). They can be understood as quasihexagonal phases which are distorted in such a way that the Cu atoms are located along the $[1\bar{1}0]$ troughs of the substrate—on or close to fourfold hollow and bridge sites. Adsorption along the $[1\bar{1}0]$ troughs not only explains the perfect order along one lattice direction in all of these structures, but also the deviations from the 60° angles between lattice directions characteristic for an ideal, hexagonal phase. The distribution of Cu atoms within these troughs is affected also by the geometry of the substrate lattice, which leads to the reduced alignment along the other lattice directions. In these phases structural rearrangements, by displacement of Cu atoms along $[1\bar{1}0]$, are relatively easy. They indeed occur between 0.25 and 0.20 V and again around 0.18 V. Finally, two different domains with the well-aligned directions oriented 90° to each other were observed for all of these phases on Au(100), as expected from the symmetry of the substrate.

The existence of Cu superstructures on Au(111) in sulfuric-acid solutions had been inferred already from the cyclic voltammograms, which show two distinct adsorption peaks around 0.22 and 0.05 V.¹¹ But even in the absence of such multiphase structures ordered adlayers may exist, as demonstrated by the present results for Cu on Au(100), where a single, broad deposition peak is reported.¹⁰ Nevertheless, pronounced structures in the current-potential curves strongly indicate structural rearrangements within the adlayer.

Ex situ RHEED and LEED investigations of Cu deposition on Au(111) yielded a $(\sqrt{3} \times \sqrt{3})R30^\circ$ pattern at medium coverages.² From our STM images (phase I) it is seen that only $\frac{1}{3}$ ML can be accommodated in this structure, whereas a coverage evaluation from the charge passing the interface would yield $\Theta \geq \frac{1}{2}$ [see Fig. 2(a) in Ref. 10]. This demonstrates the significant contribution of anions to the electrochemical current, and hence care has to be taken in coverage evaluations from current-potential curves.

The observation of a (5×5) superstructure in the STM measurements, at potentials where *ex situ* LEED studies reveal the presence of a $(\sqrt{3} \times \sqrt{3})R30^\circ$ structure, seems to be at variance with the latter results. There is experimental evidence, however, that the slow formation of a (5×5) structure in our measurements may be caused by slow, diffusion-limited coadsorption of trace impurities of Cl^- ($\leq 10^{-6} \text{ M}$), which had been demonstrated to markedly influence the deposition process of Cu.¹⁰

The good agreement between the structural results ob-

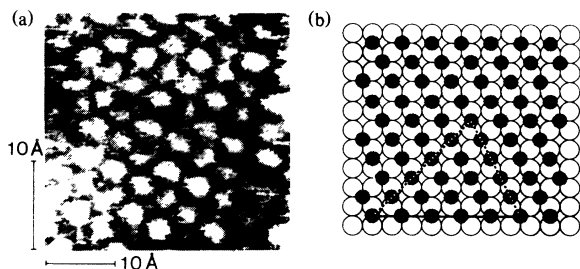


FIG. 4. Ordered structure of a Cu adlayer on Au(100) in 0.05 M $\text{H}_2\text{SO}_4 + 5 \text{ mM CuSO}_4$, at $U_{\text{SCE}} = 0.20 \text{ V}$. (a) STM image ($U_i = -60 \text{ mV}$, $I_i = 250 \text{ nA}$); (b) model of the adlayer structure (open circles: Au atoms in the topmost layer; filled circles: Cu adatoms; solid line: well-aligned Cu atoms along $[1\bar{1}0]$; dashed lines: less-ordered adlayer lattice directions).

tained by such different methods as *in situ* STM and *ex situ* LEED lends further credibility to these data. It demonstrates that the $(\sqrt{3}\times\sqrt{3})R30^\circ$ structure is a genuine structure of the interface and neither results from the absence of bulk electrolyte after emersion (important for *ex situ* techniques) nor from tip-surface interactions in the STM measurement. This statement can certainly be generalized to all Cu structures observed in this study. Apparently no new adlayer structures are induced by the presence of the tip, which is in good agreement with experiences for STM measurements at the surface-vacuum interface.

Together with the (1×1) structure for the full monolayer, which was not investigated here but which had been reported before,^{2,3} the ordered structures of adsorbed Cu on Au(111) and Au(100) can be understood as a series of increasingly close-packed, quasihexagonal adlayer structures. They reflect significant interactions between the Cu adatoms, which make the arrangement in the more widely spaced structures such as the $(\sqrt{3}\times\sqrt{3})R30^\circ$ energetically most favorable. These interactions are obviously strong enough to force the adsorbed Cu atoms out of registry with the substrate, e.g., in the quasihexagonal phases on Au(100) or in the (5×5) structure on Au(111). In contrast, under vacuum conditions a Cu adlayer grows on Au(111) in islands of a pseudomorphic (1×1) phase from the very beginning.² This indicates strong attractive, "cohesive" nearest-neighbor interactions, typical for metallic adsorbates. The presence of the electrolyte thus has a pronounced influence on the adatom-adatom interactions in the Cu adlayer and consequently on its structure. The structure-determining role of anions, which has been noted on previous occasions,¹² is thus demonstrated again in this study.

In summary, we have presented atomic-resolution, *in situ* STM images of the clean and Cu-covered Au(111) and Au(100) electrode surfaces, which reveal the existence of several ordered phases for electrodeposited Cu adlayers. The observed structures indicate repulsive in-

teraction between closely spaced Cu adatoms, which is attributed to coadsorbed anions.

We are grateful to J. Wiechers for his help in the initial stages of the experiments, to the Deutsche Forschungsgemeinschaft (Sonderforschungsbereich No. 128 and No. 338) for financial support of J.H. during part of his visit, and to the Alexander von Humboldt-Stiftung for a grant to R.J.N.

^(a)Permanent address: Department of Physical Chemistry and Electrochemistry, Jagiellonian University, 3 Karasia Strasse, 30-060 Krakow, Poland.

^(b)Permanent address: Fritz-Haber-Institut der Max-Planck-Gesellschaft, Faradayweg 4-6, D-1000 Berlin 33, Federal Republic of Germany.

¹D. M. Kolb, Z. Phys. Chem. **154**, 179 (1987).

²Y. Nakai, M. S. Zei, D. M. Kolb, and G. Lehmppuhl, Ber. Bunsenges. Phys. Chem. **88**, 340 (1984).

³O. R. Melroy, M. G. Samant, G. L. Borges, J. G. Gordon, L. Blum, J. H. White, M. J. Albarelli, M. McMillan, and H. D. Abreuña, Langmuir **4**, 728 (1988).

⁴R. Christoph, H. Siegenthaler, H. Rohrer, and H. Wiese, Electrochim. Acta **34**, 1011 (1989).

⁵M. P. Green, K. J. Hanson, D. A. Scherson, X. Xing, M. Richter, P. N. Ross, R. Carr, and I. Lindau, J. Phys. Chem. **93**, 2181 (1989).

⁶F.-R. F. Fan and A. J. Bard, J. Electrochem. Soc. **136**, 3216 (1989).

⁷J. Wiechers, T. Twomey, D. M. Kolb, and R. J. Behm, J. Electroanal. Chem. **248**, 451 (1988).

⁸J. Clavilier, R. Faure, G. Guinet, and R. Durand, J. Electroanal. Chem. **107**, 205 (1980).

⁹H. Angerstein-Kozłowska, B. E. Conway, A. Hamelin, and L. Stoicoviciu, Electrochim. Acta **31**, 1051 (1986).

¹⁰D. M. Kolb, K. Al Jaaf-Golze, and M. S. Zei, in DEHEMA-Monogr. **102**, 53 (1986).

¹¹J. W. Schultze and D. Dickertmann, Surf. Sci. **54**, 489 (1976).

¹²M. S. Zei, G. Qiao, G. Lehmppuhl, and D. M. Kolb, Ber. Bunsenges. Phys. Chem. **91**, 349 (1987).

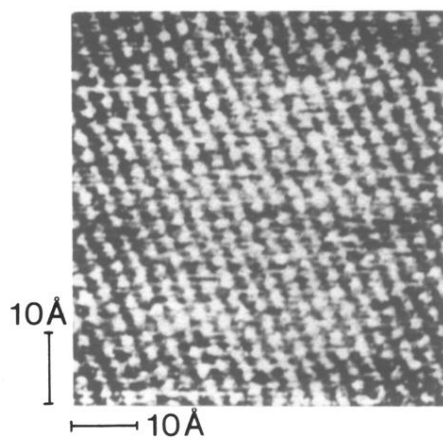


FIG. 1. Atomic-resolution STM image of the clean, unreconstructed Au(100) surface in 0.05 M H_2SO_4 +5 mM CuSO_4 (atomic corrugation 0.5 Å, $U_t = -60$ mV, $I_t = 250$ nA, $U_{\text{SCE}} = 0.3$ V).

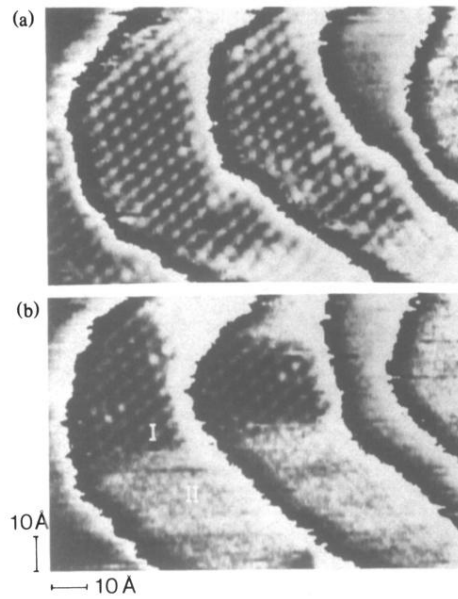


FIG. 2. STM images of a Cu-covered Au(111) surface in 0.05 M $\text{H}_2\text{SO}_4 + 5$ mM CuSO_4 , taken on the same area at slightly different potentials. (a) $U_{\text{SCE}} = 0.215$ V; (b) $U_{\text{SCE}} = 0.20$ V. Two Cu adlayer structures—a strongly corrugated $(\sqrt{3} \times \sqrt{3})R30^\circ$ and a weakly corrugated (5×5) —coexist on the surface ($U_t = -170$ mV, $I_t = 2.5$ nA, phases I and II as indicated).

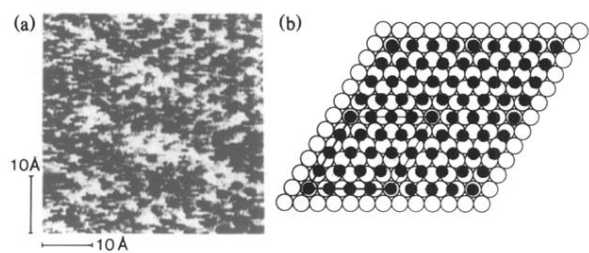


FIG. 3. (5×5) structure of a Cu adlayer on Au(111) in $0.05 \text{ M H}_2\text{SO}_4 + 5 \text{ mM CuSO}_4$ at $U_{\text{SCE}} = 0.20 \text{ V}$. (a) STM image ($U_t = -100 \text{ mV}$, $I_t = 100 \text{ nA}$); (b) model of the adlayer structure (O: Au atoms in the topmost layer; ●: Cu adatoms).

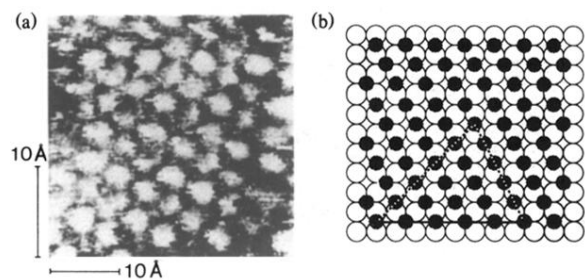


FIG. 4. Ordered structure of a Cu adlayer on Au(100) in 0.05 M H_2SO_4 +5 mM CuSO_4 , at $U_{\text{SCE}}=0.20$ V. (a) STM image ($U_t = -60$ mV, $I_t = 250$ nA); (b) model of the adlayer structure (open circles: Au atoms in the topmost layer; filled circles: Cu adatoms; solid line: well-aligned Cu atoms along $[1\bar{1}0]$; dashed lines: less-ordered adlayer lattice directions).